ELSEVIER

Ceramics International 29 (2003) 271–278

CERAMICS INTERNATIONAL

www.elsevier.com/locate/ceramint

Processing of porous ceramic spheres by pseudo-double-emulsion method

Jung Shick Lee, Jai Koo Park*

Department of Geoenvironmental System Engineering, Hanyang University, 17, Heangdang-dong, Seongdong-gu, Seoul 133-791, Republic of Korea

Received 18 February 2001; received in revised form 5 April 2002; accepted 5 May 2002

Abstract

A process for the fabrication of porous ceramic spheres for microorganism carriers is described. A new fabrication method for the process was developed using simple gelcasting and bubble-in-water-in-oil type of pseudo-double-emulsion. The globules, consisting of a foamed mullite suspension, were dispersed and consolidated in spherical shape in liquid paraffin as gelation progressed. The green spheres were pyrolysed at 600 °C and sintered at 1500 °C. The influence of surfactants, extension ratio, and impeller revolution rate on the process and characteristics of the spheres was investigated. The sphere size was in the range 1–5 mm and determined directed by impeller revolution rate. The macropore size in the case of the anionic surfactant was less than that for the cationic surfactant. The inner macropores were interconnected and extended to the external surface. The macroporosity of macropores, in the range 65–79%, increased with extension ratio.

Keywords: Porous; Ceramic sphere; Gelcasting; Double-emulsion

1. Introduction

Porous ceramics and polymeric foams have been used as microorganism carriers, called biomedia, in biological wastewater treatments [1–3] and fermentation processes [4]. As pollutants have become more toxic and varied, the need for pertinent materials with advanced properties has been increasing significantly to meet the stringent requirements of newly developed environmental processes. Recently, interest in ceramic biomedia has risen by virtue of their excellent properties of chemical inertness, high durability, and lack of clogging [5]. Moreover, microorganisms can immobilize more easily and strongly on the rough surface of ceramic biomedia than polymeric biomedia [6].

So far, numerous routes for the preparation of porous ceramics, such as foaming [7], partial sintering of particles [8], aerogel processing of sol-gel materials [9], and percolating pyrolyzable particles [10] have been developed since Schwartzwalder's and Somers' initial work [11]. The methods can be divided into two groups according to pore structure: one is a foam structure, in which closed pores are dispersed in the matrix; the other is a reticulate structure, in which open pores are interconnected through channels. Both porous ceramics of foam and reticulate structures can be obtained by foaming method since the foam structure is altered gradually into the reticulate structure with increasing porosity. The foaming method has some distinguishing features in that it allows easy control of pore structure (porosity, pore size, and pore type). It is expected that porous ceramics, prepared by the foaming method, would possess an optimal pore structure for carrying various kinds of microorganisms in the terms of two points: One is high surface area, which provides site for microorganism adsorption and the other is interconnected pores for mass transfer between microorganisms within inner pores and the substrate in the external phase. On the other hand, the foaming method for highly porous ceramics has fabrication shortcomings due to cracking during drying and low green strength. Sepulveda and Binner [7] employed the gelcasting method of Young et al. [12] of in-situ polymerization of organic monomers for fabrication of foamed suspensions. This method required inert gas for generating

* Corresponding author.
E-mail address: jkpark@hanyang.ac.kr (J.K. Park).

0272-8842/03/$22.00
PII: S0272-8842(02)00115-3

bubbles and many additives, such as initiator, monomer, cross-linker, and catalyst. In the present work, a simple gelation reaction, cross-linking between two water-soluble polymers, was used for gelcasting.

A spherical shape for porous ceramics is preferable in the case of specific biomedia used in fluidized bed biological processes [3] because spheres can be uniformly suspended and can reduce breakage loss by collision. Nevertheless, reports of the preparation of porous ceramic spheres (PCS) are infrequent because conventional ceramic fabrication methods, such as granulation by vibration, spraying, or molding, do not yield porous spheres with suitable properties. While control of the characteristics (sphere size, porosity, pore size, and pore type) that influence the performance is a prerequisite for some applications, the existing methods also have limitations in controlling the pore structure.

In the present work, a novel process for the fabrication of porous ceramic spheres (PCS) using mechanical foaming of aqueous ceramic suspensions and air-in-water-in-oil type of pseudo-double-emulsions is described.

2. Pseudo-double-emulsion

Fig. 1 shows a schematic representation of a pseudo-double-emulsion (PDE) from a three-phase foamed suspension (3PFS). The double-emulsion method has been developed in the pharmaceutical industry for preparing microspheres for the impregnation of medicines [13]. Foaming can be considered to be a type of emulsification since the two are very similar. In order to produce a PDE, a 3PFS is re-emulsified, as in the case of an oil-in-water-in-oil type of double-emulsion [14]. In this PDE, constituent bubbles are the first dispersed phase, globules are the second dispersed phase, a mullite suspension is the first continuous phase, and oil is the second continuous phase. That is to say, the globules of 3PFS, dispersed in the second continuous phase, contain an even smaller dispersed phase within themselves.

When a PDE is produced, globules of a 3PFS are divided into daughter ones by the shear of the second continuous phase and the globules coalesce simultaneously into larger ones by collision among themselves. The globule size is determined by the disruption and coalescence rates [15]. Hence, the major factor influencing the globule size and the disruption behavior is the ratio of the viscosity of the second dispersed phase ($\eta_{\text{dispersed}}$) to that of the second continuous phase ($\eta_{\text{continuous}}$). The external stress, induced by the shear of the second continuous phase flow, acts on the interface of the globule. If the external stress exceeds the interfacial tension and the internal stress originating from the globule viscosity, the globule is distorted into a prolate ellipsoid and is divided finally into daughters. Fig. 2 shows representative example of disruption behavior of globules in shear for various viscosity ratios ($\eta_{\text{dispersed}}/\eta_{\text{continuous}}$) [16]. Fig. 2 suggests that the viscosity ratio must be larger than 1.0 for globules to exist in spherical shape in a PDE.

An oil-soluble surfactant, which adsorbs onto the interface between oil and water, is used generally for interrupting coalescence of aqueous globules by steric hindrance in a water-in-oil emulsion. Such a surfactant was not added in present work because the purpose was to produce a coarse emulsion consisting of the globules of millimeter size.

3. Experimental procedure

3.1. Processing of porous ceramic spheres

Fig. 3 shows a flow chart for the overall process, which consists of suspension preparation, foaming by

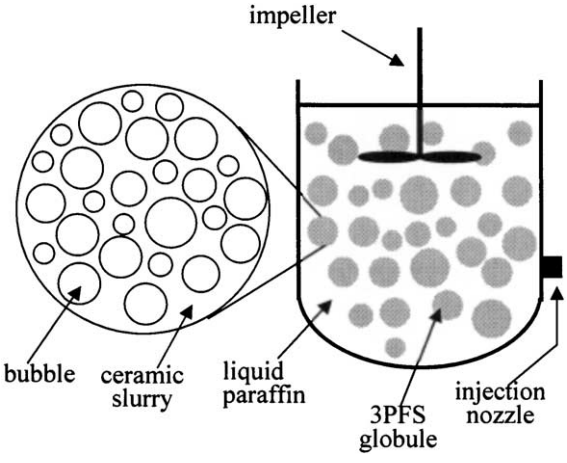

Fig. 1. Schematic representation of a PDE including globules of a 3PFS and the reactor.

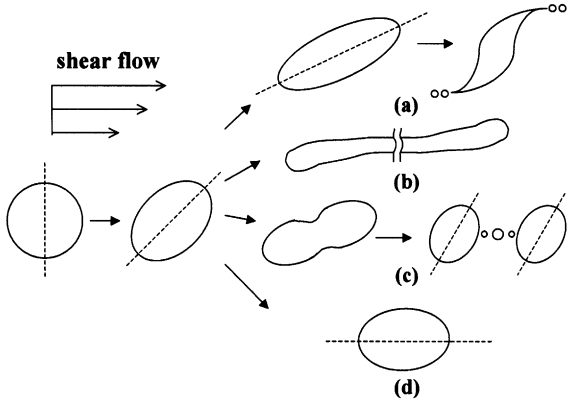

Fig. 2. Representative disruption behavior of globules for various viscosity ratios in simple shear flow: viscosity ratio (a) 0.0002, (b) 0.7, (c) 1.0, (d) 6.0.

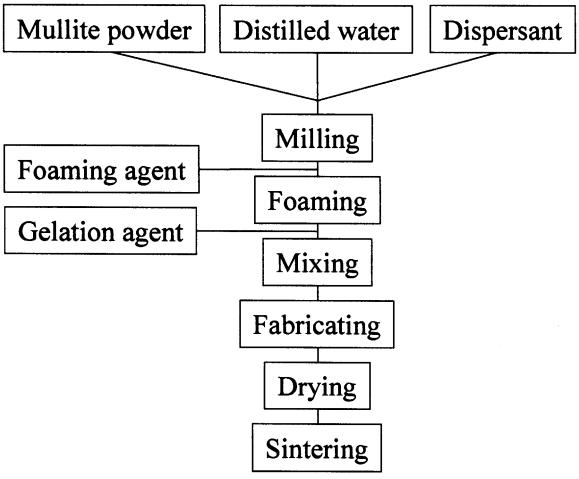

Fig. 3. Flow chart for preparing PCS using the PDE method.

mechanical whisking, fabricating, drying, and sintering. Aqueous suspensions, containing 45 vol.% mullite powder (Koyritsu Ceramic Materials Co. Ltd., Japan) and 3.5 wt.% dispersant of polyethyleneimine (PEI, Lupasol-HF, BASF Co. Ltd., Germany), were prepared by attrition milling (KMD-1B, Korea Material Development Co. Ltd., Korea) for 4 h.

Cationic and anionic surfactants (CTAC-29 and T-435, respectively, Miwon Chemical Co. Ltd., Korea) were used individually as a foaming agent and added to the mullite suspension of 100 cm^3 at the level of 0.5 wt.%. The suspensions were whisked vigorously with a food mixer with two rotors at a whisking rate of 900 rpm in a plastic beaker of 500 cm^3 in order to prepare 3FPS of 250, 300, 350, 400, and 450 cm^3. Then, each 3PFS was whisked at 600 rpm for 30 s. Next, the gelation agent (Denacol-EX614B, Nagase Chemicals Co. Ltd., Japan) at the level of 1.2. wt.% was added to the 3PFS during whisking at 600 rpm for a further 30 s.

The reactor for the PDE was an acrylic cylinder (180 mm in diameter and 180 mm in height) with hemispherical bottom (180 mm in diameter and 80 mm in height) filled with 4 l of liquid paraffin (second continuous phase). An impeller, which had four wings of 70 mm length and 20 mm width, was located in the liquid paraffin. 3PFS of 250 cm^3 was injected into the reactor by a peristaltic pump at a constant impeller revolution rate during the fabricating process to produce a PDE. The injection rate was 12.5 cm^3/s. Stirring was done at impeller revolution rates of 120, 140, 160, 180, 200, 220, and 240 rpm for 1 h. The green spheres were separated by sieving from the liquid paraffin, followed by drying in air at 80 °C for 6 h. Pyrolysis of the dried green spheres was carried out in an alumina crucible at 600 °C in air for 2 h and sintering of the pyrolysed spheres was performed with an electric furnace (51314, General Signal Co., UK) at 1500 °C for 2 h using heating rates of 100 °C/h up to 600 °C and then 200 °C/h up to the final temperature in air.

3.2. Rheological behavior

The viscosities of the mullite suspensions, 3FPS, and liquid paraffin at varying shear rates were measured at 26 °C with a cylindrical viscometer (RV-DV II+, Brookfield Co., USA). Shear rates were in the range 1–70 s^{-1}. Since the bubbles in the suspension had a significant effect on the suspension viscosity, the suspension was placed under vacuum for 10 min at 60 mm Hg for degassing before measuring. On the other hand, the viscosities of the 3PFS were measured immediately after the foaming process. The viscosities of the mullite suspensions, after adding the gelation agent, were measured to determine the induction period leading to the onset of gelation.

3.3. Characterization of porous ceramic spheres

The size distribution of the sintered PCS was measured by sieve analysis. US standard sieves in the range 0.297–4.760 mm were used. The bulk densities of the PCS were obtained by measuring the dimensions of specimens for the calculation of true porosities. The pore size distributions of the PCS were characterized by image analysis (Image-Pro Plus ver. 4.0, I&G Plus, USA) from sectioned PCS using an optical microscope [17]. The pore structures were observed by scanning electron microscopy (JSM-6300, JEOL Co., Japan). The specific surface areas of the PCS were measured by the N_2 gas adsorption method (Nova1000, Quantachrome Co., USA).

4. Results and discussion

4.1. Processing of porous ceramic spheres

Fig. 4 shows the viscosity of the mullite suspension with the PEI as a polymeric dispersant. The viscosity decreased with increasing shear rate and approached just over 100 cp above shear rate of 30 s^{-1}. Fujiu et al. [18] reported that a suitable viscosity was more or less 100 cp for the foaming process for ceramic suspensions. The suspension prepared in present work had a sufficiently low viscosity since the shear rate, which was induced by vigorous stirring in order to incorporate air into the mullite suspension, can be assumed to have been certainly higher than 30 s^{-1}. However, the PEI is not a well-known dispersant; it was selected in order to consolidate the 3PFS. Imine radicals, which branch from the PEI, cross-linked with epoxy radicals from the gelation agent added during the foaming process. As a result of the cross-linking, the PEI and the gelation

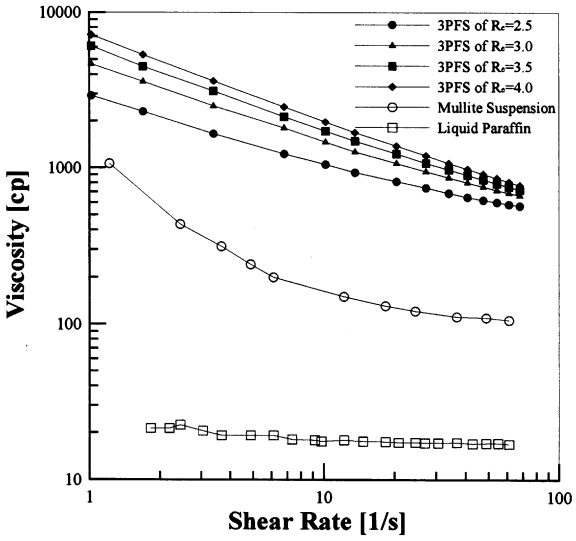

Fig. 4. Viscosities of the mullite suspension, liquid paraffin, and 3PFS at various extension ratios (R_e) as a function of shear rate.

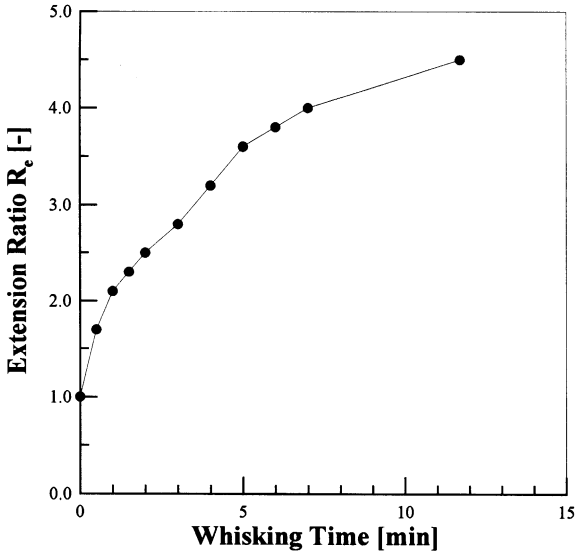

Fig. 5. Extension ratio R_e of the 3PFS with the cationic surfactant as a function of whisking time at 900 rpm.

agent created a three-dimensional tangled network, consolidating the 3PFS. The PEI was employed successfully in order to prepare the mullite suspension for the foaming process.

The viscosity of the 3PFS (second dispersed phase) at various extension ratios (R_e) and the liquid paraffin (second continuous phase) versus shear rate at 26 °C are shown in Fig. 4. The R_e is the ratio of the volume of the 3PFS to that of the initial suspension. The liquid paraffin revealed Newtonian behavior and its viscosity was 17 cp. It was inferred that disruption motion according to Fig. 2(c or d) occurred because the viscosity ratios of the 3PFS at all R_e to the liquid paraffin were significantly high. Furthermore it could be expected from the viscosity ratios of the 3PFS that green spheres were spherical shape. This expectation coincided with following result.

Fig. 5 shows the R_e versus whisking time at 900 rpm in foaming process. The R_e increased with whisking time, requiring 2.0, 3.5, 4.8, 7.0, 11.7 min to prepare a 3PFS of $R_e = 2.5$, 3.0, 3.5, 4.0, 4.5, respectively. This occurred because air becomes entrapped in the turbulent suspension and the surfactant solution is drawn around each bubble during whisking at 900 rpm [7]. It was observed during whisking at 600 rpm that the 3PFS volume showed no further increase and that large bubbles of millimeter size disappeared. It was considered that whisking at low rpm was required to homogenize the suspension for a constant bubble size. Uniform bubbles created a uniform pore structure since they were converted into pores during the processing.

A 3PFS injected into the reactor is divided into several lumps during emulsification. The lumps were broken quickly into smaller liquidlike globules by the flow of the liquid paraffin at $R_e = 2.5$–4.0. When R_e was 4.5 at all impeller revolution rates and $R_e = 3.0$–4.0 at 120 rpm, the 3PFS could not be dispersed because most of the injected 3PFS floated on the liquid paraffin. Fast impeller revolution rates are needed to disperse 3PFS of large density difference in a medium (second continuous phase). These high rates cause high shear forces, which squeeze the constituent bubbles from liquidlike globules. $R_e = 4.5$ and 120 rpm were incongruous experimental conditions in the present work.

The emulsification consisted of two stages. The globule size was varied continuously by disrupting and coalescing in the first stage. Although disruption appears to predominate over coalescence in this stage, it can be inferred by considering the disruption mechanism of a globule as mentioned above that there is the reversion point when the coalescence rate surpasses the disruption rate and liquidlike globule size increases. While two rates could be calculated by measuring the globule size distribution with time, the size variation could not be obtained in the present work because globule size was too coarse to measure by commercial particle size analyzers. Nevertheless, the behavior can be explained as follows. As the globule becomes viscous and adhesive by gelation, the internal force from viscosity increases and resists the external force induced by the flow, so disruption hardly occurs and the globule can maintain its shape. Fig. 6 shows the viscosity of the mullite suspension as a function of time after the addition of the gelation agent. The induction period was 5 min. The viscosity of the mullite suspension (first continuous phase), determining the viscosity of a 3PFS, rose sharply after 10 min. Hence it was found that the reversion point was established after 10 min.

In the second stage of emulsification, the globules hardened into green spheres as the gelation reaction

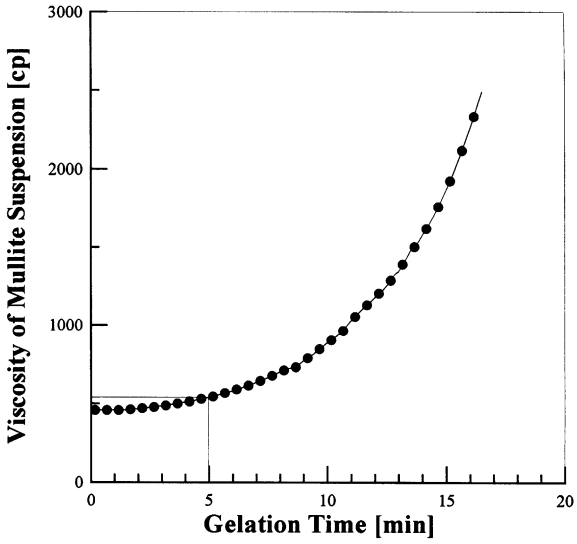

Fig. 6. Viscosity of the mullite suspension after addition of the gelation agent as a function of time.

progressed within them. Wet green spheres, separated after gelation of 25 min in a PDE, agglomerated into clusters. However, agglomeration was not observed in the wet green spheres after gelation of 40 min, the wet green spheres did not maintain a spherical shape in a pile due to their weight. Agglomeration and collapse of the green spheres were not observed after gelation of 1 h. It was found that gelation time of 1 h was required to obtain the green spheres of sufficient strength to be separated from the liquid paraffin and to be handled for the following processes.

Recovery was 98%, which was determined by measuring the weight of mullite powder for all samples. The loss of 2% resulted from the globules' adhering to the reactor surface. Damage and loss were not detected in drying, pyrolysis, or sintering. The results demonstrate that the foaming method allowed successful the gelation and the PDE in order to prepare PCS.

4.2. Size distribution of sintered spheres

Fig. 7 shows PCS prepared at different impeller revolution rates for $R_e = 2.5$ and 4.0 using the process described above. The PCS were spherical as expected above. Fig. 8 shows size distributions of the PCS prepared at $R_e = 3.5$ for various impeller revolution rates. The PCS were distributed in the range 1–5 mm. Fig. 9 shows mean sizes of the PCS as a function of the impeller revolution rate for various R_e. The mean size decreased generally with the increasing impeller revolution rate. In the case of $R_e = 3.5$, the mean size was varied in the range 2.5–4.0 mm. At all impeller revolution rates, the mean sizes of PCS prepared at $R_e = 2.5$ were smaller than those at other R_e values. There was no clear influence of the R_e on the mean size in the range

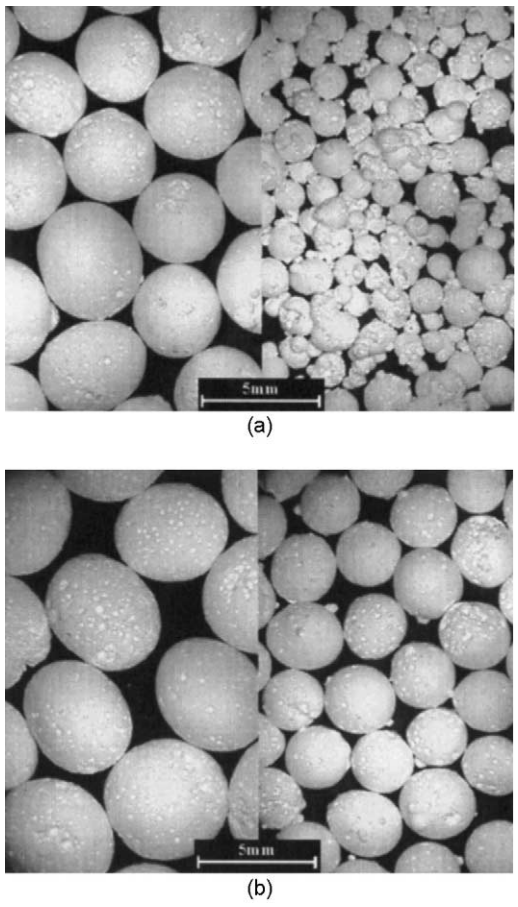

Fig. 7. Porous ceramic spheres prepared at (a) $R_e = 2.5$ (left: at 140 rpm, right: at 220 rpm) and (b) $R_e = 4.0$ (left: at 140 rpm, right: at 220 rpm).

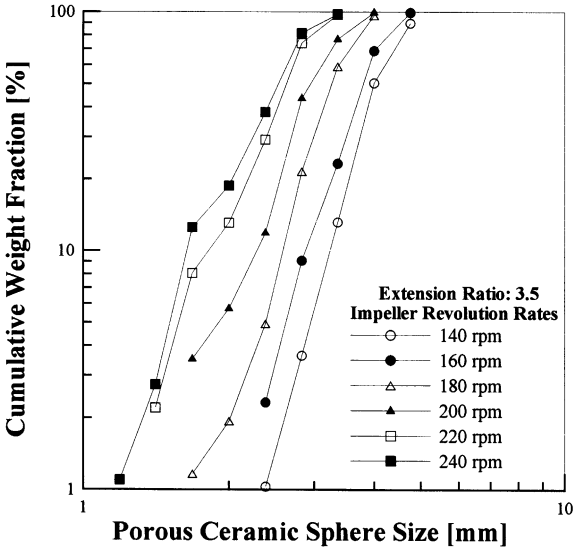

Fig. 8. PCS size distributions at $R_e = 3.5$ for various impeller revolution rates.

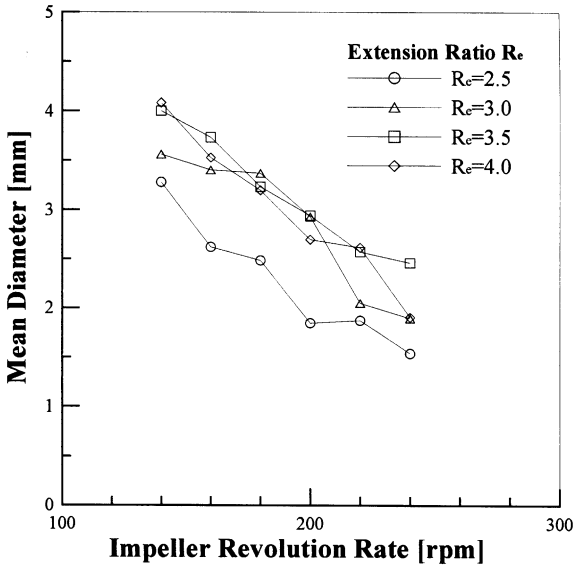

Fig. 9. Mean size of PCS as a function of impeller revolution rate for various R_e.

$R_e = 3.0$–4.0. When the R_e was in the range 3.0–4.0, the liquidlike globules were not homogeneously dispersed and were concentrated in the upper layer of the reactor due to buoyancy. These globules had greater chance of coalescing than those produced at $R_e = 2.5$. It is found that sphere size can be controlled easily by the impeller revolution rate in the above range.

4.3. Pore structure of porous ceramic spheres

True and apparent porosities, average pore size, pore size distribution, pore shape, and permeability are the relevant microstructural factors for the present application. Fig. 10 shows the pore structure of the PCS with the cationic surfactant (CTAC-29) as a foaming agent. The PCS has a bimodal pore size distribution consisting of macropores (a and b) and micropores less than 2 μm in size (c). The macropores originated from the constituent bubbles and the micropores were formed from interstices between the mullite particles during partial sintering. Fig. 11 shows the macropore size distributions of the PCS with different foaming agents. The macropores were in the diametral size range 50–400 and 30–200 μm for the cationic and the anionic surfactants, respectively. This difference indicates that the macropore size can be controlled with foaming agents. Foams using anionic surfactants generally are more stable than those using cationic types [19]. The more unstable the foam is, the more enlarged the constituent bubbles become by two major mechanisms: coalescence due to lamellar thinning behavior and gas diffusion due to pressure gradient. Consequently, pores, which reveal the contour of the constituent bubbles, also become enlarged. Some studies have reported that the preferable pore size of ceramic carriers is more than five times of the diameter of the microorganisms [4,20]. The present

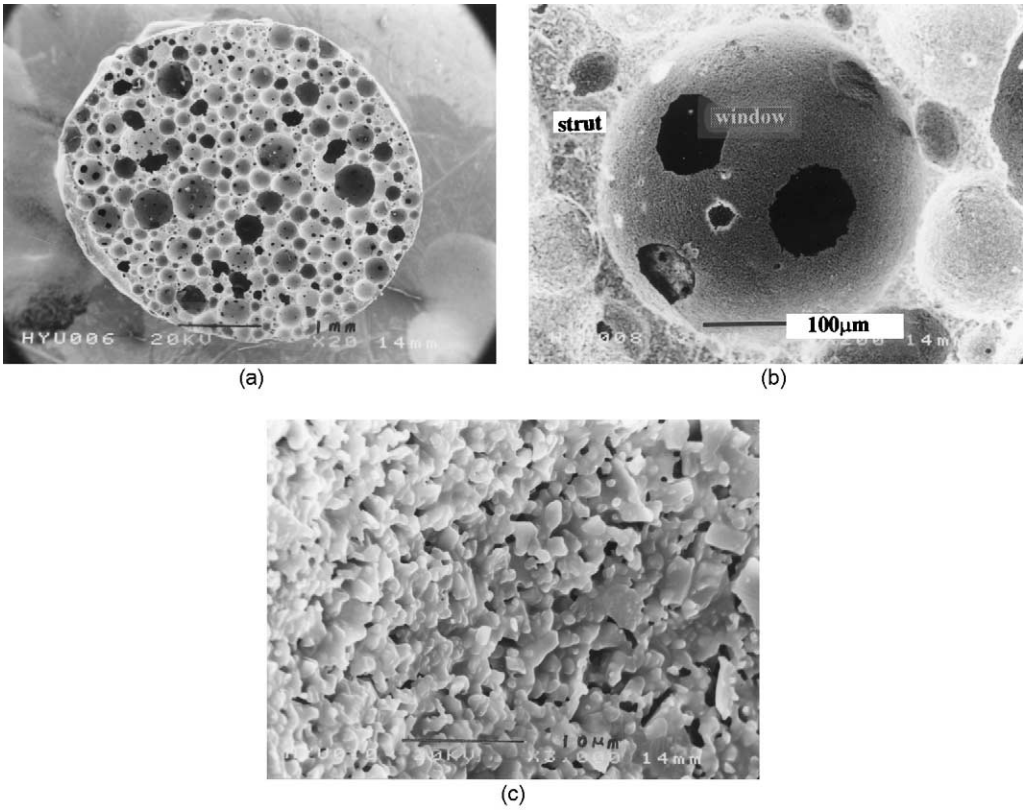

Fig. 10. Pore structure of the PCS with the cationic surfactant (CTAC-29): (a) cross-section, (b) open macropore, and (c) micropore in strut.

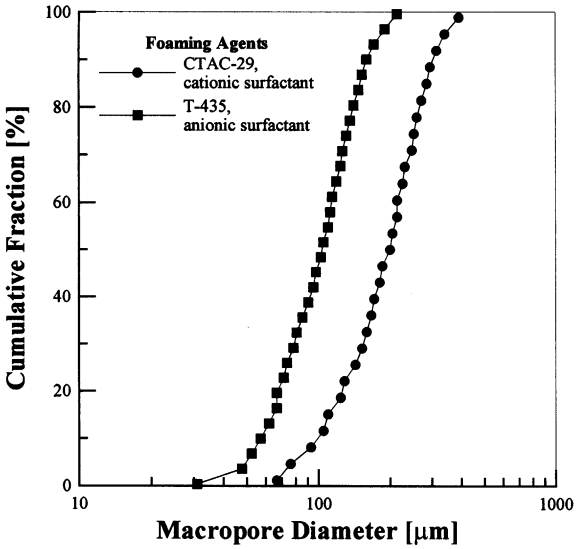

Fig. 11. Pore size distribution of the PCS with cationic (CTAC-29) and anionic (T-435) surfactants by image analysis.

PCS has a suitable macropore size distribution [21,22] since the size range of microorganism associated with wastewater treatment is in the range 1–50 μm [6].

Fig. 12 shows the external surface of a PCS, which shows many open macropores. They formed when bubbles were released from liquidlike globules in the PDE. The inner macropores are interconnected to each other and the external surface through windows [Fig. 10(b)]. The channeling developed with increasing porosity, as mentioned previously.

The true porosities of the PCS (ε_{true}), consisting of the macroporosity (ε_{macro}, pore sizes above 10 μm) and the microporosity (ε_{micro}, pore sizes below 2 μm), calculated from the bulk densities of the PCS were 75, 80, 83, and 85% at $R_e = 2.5$, 3.0, 3.5, and 4.0, respectively. This result indicates that the true porosity can be controlled directly by the R_e during the foaming process. The ε_{macro} and the ε_{micro} can be also calculated from the ε_{true} and the ε_{strut}, which is the specific true porosity of the strut, by means of the following equations:

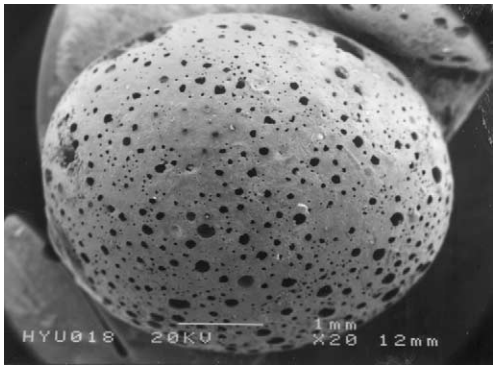

Fig. 12. Micrograph of the external surface of a sintered PCS.

$$\varepsilon_{macro} = \frac{\varepsilon_{true} - \varepsilon_{strut}}{1 - \varepsilon_{strut}}, \quad \varepsilon_{micro} = \varepsilon_{true} - \varepsilon_{macro} \tag{1}$$

The ε_{strut} of 0.29 was obtained by measuring the bulk density of a specimen prepared by the process in Fig. 3 with the gelcasting and without the foaming and the PDE processes. The ε_{macro} were 65, 72, 76, and 79% at $R_e = 2.5$, 3.0, 3.5, and 4.0, respectively. Apparent porosity ($\varepsilon_{apparent}$) is more important than the ε_{true} in the present application because open macropores are available for the microorganism adsorption. The $\varepsilon_{apparent}$ can be substituted by the ε_{macro} in the present work since almost all the macropores are interconnected by windows.

The specific surface areas of the PCS were in the range 2.0–4.5 m^2/g. Although microporous materials, such as activated carbons and zeolites, have high specific surface areas, their pores less than 10 nm in diameter are not effective for the microorganism adsorption. All PCS, prepared at all impeller revolution rates, had no significant difference in pore structure. It is expected from the observation of the pore structure that the PCS at $R_e = 4.0$ would show the best performance as biomedia in light of their adsorption capacity for microorganisms and channeling.

5. Conclusions

The gelation with water-soluble polymers and a PDE consisting of 3PFS globules were used with a mechanical foaming method in order to fabricate porous green spheres. A 3PFS, prepared by mechanical whisking, was emulsified simply in liquid paraffin by stirring under the proper conditions. PCS sizes were in the range 1–5 mm and the size could be controlled by the impeller revolution rate. The PCS showed a desirable pore structure, high macroporosity in the range 65–79%, and interconnected macropores in the size range 30–400 μm. The porosity and the macropore size of the PCS were controlled by the R_e and the type of surfactant, respectively. The present work has shown that the fabrication method is combined successfully to the conventional mechanical foaming process for porous ceramic spheres with clear advantages in terms of being able to control the sphere size, the porosity, and the macropore size.

References

[1] K. Breitenbûcher, M. Siegal, A. Knûpfer, M. Radke, Open-pore sintered glass as a high-efficiency support medium in bioreactors: new results and long-term experiences achieved in high-rate anaerobic digestion, Water Sci. Tech. 22 (1990) 25, 32.
[2] N. Hashimoto, T. Sumino, Wastewater treatment using activated sludge entrapped in polyethylene glycol prepolymer, J. Fermentation Bioeng. 86 (1998) 424–426.
[3] J.J. Heijnen, A. Mulder, R. Weltevrede, J. Hols, H.L.J.M. Van

Leeuwen, Large scale anaerobic-aerobic treatment of complex industrial waste water using biofilm reactors, Water Sci. Tech. 23 (1991) 1427–1436.
[4] S. Furuta, H. Katsuki, Modification of porous silica with activated carbon and its application for fixation of yeasts, J. Porous Mater. 8 (2001) 43–48.
[5] T.D. Kent, C.S.B. Fitzpatrick, S.C. Williams, Testing of biological aerated filter (BAF) media, Water. Sci. Tech. 34 (1996) 363–370.
[6] W.G. Characklis, K.C. Marshall, Biofilms, John Wiley and Sons, New York, 1989.
[7] P. Sepulveda, J.G.P. Binner, Processing of cellular ceramics by foaming and in situ polymerisation of organic monomers, J. Eur. Ceram. Soc. 19 (1999) 2059–2066.
[8] M. Wismer, Inorganic Foams, Marcel Dekker, New York, 1973.
[9] M.M. Santos, W.L. Vasconcelos, Properties of porous silica glasses prepared via sol–gel process, J. Non-Cryst Solids 273 (2000) 145–149.
[10] K. Maca, P. Dobsak, A.R. Boccaccini, Fabrication of graded porous ceramics using alumina–carbon powder mixtures, Ceram. Int. 27 (2001) 577–584.
[11] K. Schwartzwalder, A.V. Somers, US patent 3 090 094, 21 May 1963.
[12] C. Young, O.O. Omatete, M.A. Janney, P.A. Mnchhofer, Gelcasting of alumina, J. Am. Ceram. Soc. 74 (1991) 612–618.
[13] T. Ehtezazi, C. Washington, C.D. Melia, Determination of the internal morphology of poly (D, L-lactide) microspheres using stereological methods, J. Controlled Release 57 (1999) 301–314.
[14] N. Garti, Double emulsions — scope, limitations and new achievements, J. Coll. Surf 123 (1997) 233–246.
[15] V. Mishra, S.M. Kresta, J.H. Masliyah, Self-preservation of the drop size distribution function and variation in the stability ratio for rapid coalescence of a polydisperse emulsion in a simple shear field, J. Coll. Interf. Sci. 197 (1998) 57–67.
[16] H.N. Stein, The Preparation of Dispersions in Liquids, Marcel Dekker, New York, 1996.
[17] J.K. Park, S.H. Lee, Observation and segmentation of gray images of surface cells in open cellular ceramic foams, J. Ceram. Soc. Japan 109 (2001) 580–586.
[18] T. Fujiu, G.L. Messing, W. Huebner, Processing and properties of cellular silica synthesized by foaming sol–gels, J. Am Ceram. Soc. 73 (1990) 85–90.
[19] R.K. Prud'homme, S.A. Khan, Foams, Marcel Dekker, New York, 1996.
[20] R.A. Messing, R.A. Oppermann, Pore dimensions for accumulating biomass. I. Microbes that reproduce by fission or by budding, Biotechnol. Bioeng. 21 (1979) 49–58.
[21] J.H. Tay, S. Jeyaseelan, K.Y. Show, Performance of anaerobic packed-bed system with different media characteristics, Water Sci. Tech. 34 (1996) 453–459.
[22] K.Y. Show, J.H. Tay, Influence of support media on biomass growth and retention in anaerobic filters, Water Res. 33 (1999) 1471–1481.